

Special Section: Hydrological Observatories

Core Ideas

- Water quality and stream flow have temporal and spatial trends in response to variable climate.
- Our work reveals how Sierra Nevada forests responded to and recovered from multiyear drought.
- Regolith thickness trends reveal water storage capacity differences with elevation.
- Monitoring shows deep-water changes via plant utilization or capillary flow during drought.

A. O'Geen, P. Hartsough, S. Devine, Z. Tian, R. Ferrell, and J.W. Hopmans, Dep. of Land, Air and Water Resources, Univ. of California, Davis, CA 95616; M. Safeeq, E. Stacy, and R. Bales, School of Engineering, Univ. of California, Merced, CA 95343; J. Wagenbrenner, US Forest Service, Pacific Southwest Research Station, Arcata, CA 95521; M. Goulden, Dep. of Earth System Science, Univ. of California, Irvine, CA 92697. *Corresponding author (atogeen@ucdavis.edu).

Received 20 Apr. 2018.

Accepted 24 Aug. 2018.

O'Geen, A., M. Safeeq, J. Wagenbrenner, E. Stacy, P. Hartsough, S. Devine, Z. Tian, R. Ferrell, M. Goulden, J.W. Hopmans, and R. Bales. 2018. Southern Sierra Critical Zone Observatory and Kings River Experimental Watersheds: A synthesis of measurements, new insights, and future directions. *Vadose Zone J.* 17:180081. doi:10.2136/vzj2018.04.0081

© Soil Science Society of America.
This is an open access article distributed under the CC BY-NC-ND license
(<http://creativecommons.org/licenses/by-nc-nd/4.0/>).

Southern Sierra Critical Zone Observatory and Kings River Experimental Watersheds: A Synthesis of Measurements, New Insights, and Future Directions

Anthony (Toby) O'Geen*, Mohammad Safeeq, Joseph Wagenbrenner, Erin Stacy, Peter Hartsough, Scott Devine, Zhiyaun Tian, Ryan Ferrell, Mike Goulden, Jan W. Hopmans, and Roger Bales

Sensor networks within the Southern Sierra Critical Zone Observatory (SSCZO) and Kings River Experimental Watersheds (KREW) document changes in the water cycle spanning the west slope of the southern Sierra Nevada in California. The networks were established to document water dynamics throughout the critical zone spanning profile, hillslope, catchment, and watershed scales at key locations that reflect systematic differences in bioclimatic conditions imposed by a strong elevation gradient. The critical zone observatory attempts to constrain the hydrologic budget via representative measurements of streamflow, eddy flux covariance, snow depth, meteorological conditions, and water content and water potential in soil and deep regolith. These measurements reveal the complexity of interactions among all aspects of the water balance (runoff, storage, evapotranspiration [ET], and precipitation) through daily, seasonal, and annual timescales. Multiyear drought, catastrophic wildfires, insect outbreaks, and disease have caused widespread tree mortality in the Sierra Nevada. These disturbances offer a window into the future for this region, which is expected to undergo significant change in response to global warming. This hydrological observatory provides valuable hydrometric attributes and fluxes across the stream–groundwater–vadose zone–soil–vegetation–atmosphere continuum.

Abbreviations: ET, evapotranspiration; KREW, Kings River Experimental Watersheds; MAP, mean annual precipitation; MAT, mean annual temperature; NADP, National Atmospheric Deposition Program; PAW, plant-available water holding capacity; SSCZO, Southern Sierra Critical Zone Observatory; SSURGO, Soil Survey Geographic database; WB, weathered bedrock; WY, water year.

The Sierra Nevada provide water to over 10% of the US population and ~40% of the runoff for California. Most of California has a massive demand for storage of precipitation provided by the montane snowpack because the population and agricultural industry are situated in semiarid or arid areas where the majority of annual precipitation occurs during fall and winter. Thus, much of the demand for water relies on reservoirs filled by runoff from Sierra Nevada snowmelt (Null et al., 2010). Gradual melting of snowpack is critical to effective operation of downstream reservoirs and use of runoff. In light of climatic uncertainties, there is an imminent need to understand current hydrologic processes in the Sierra Nevada and to forecast hydrologic response to changing climate (Howat and Tulaczyk, 2005; Bales et al., 2006).

The hydroclimatic regimes of California are characterized by high temporal variability at seasonal and interannual scales, reflecting dramatic precipitation differences associated with Mediterranean climate as well as impacts of longer-term cyclical phenomena such as El Niño–Southern Oscillation and Pacific Decadal Oscillation. Topography and land surface conditions also contribute to spatial variability across the state, where the Sierra Nevada has a substantial impact on the amount, type, and timing of precipitation. A small number of exceptional winter storms, also known as “atmospheric rivers,” can

provide the bulk of the annual precipitation (Dettinger, 2011). As a result, short- and long-term precipitation deficits are common (Griffin and Anchukaitis, 2014). California is also characterized by strong spatiotemporal variability in precipitation phase (snow vs. rain) that determines when and how much water is available for ecosystem use and runoff (Safeeq et al., 2013, 2016). Historically, ecosystems adapted to this hydroclimatic variability, in part, through a natural disturbance regime (e.g., frequent low-intensity fire), while humans attempted to manage it with built infrastructure. However, departure from the natural disturbance regime through fire suppression along with population growth and subsequent development and agriculture intensification and expansion in rangeland and forests have likely reduced California's ability to endure long-term droughts and climatic extremes.

Climate warming has and will further shift the elevation of the rain–snow transition, seasonal timing of snowmelt runoff, soil–water dynamics, growing-season temperatures, and plant water use. These effects will dramatically alter the water cycle and ecosystem processes (California Energy Commission, 2003). Snowmelt and streamflow peaks are already occurring earlier in the spring in response to warming, which has been as much as +2°C in recent decades. This rise will likely increase the risks of springtime floods (Miller et al., 2003; Das et al., 2011, 2013) and late summer moisture stress in forests (Goulden and Bales, 2014). Increased frequency of multiyear droughts and higher intensity rainfall events have been predicted and may compound the hazards associated with seasonal shifts in snow accumulation and melt.

Sierra Nevada forests have undergone significant changes in structure as a result of factors such as fire suppression, grazing, and climate change (Dolanc et al., 2014). Frequency and intensity of a range of forest disturbances—including forest die-off, large and severe wildfires, and insect outbreaks and disease—have been observed (Bales et al., 2018). The SSCZO and KREW projects were established to address a wide range of basic and applied questions through interdisciplinary science approaches. These two colocated complementary long-term research efforts serve as a unique model to advance earth system science and develop and evaluate management solutions to pressing environmental problems.

◆ Motivation and Science Questions

The overall goals of the SSCZO are stated as follows: (i) expand process-based understanding of the critical zone within a landscape that is crucial to California's social and environmental wellbeing; (ii) provide a platform for long-term physical, biogeochemical, and ecological studies; and (iii) develop a framework for improving Earth system models. The KREW has the following complementary goals: (i) quantify the natural variability in physical, biological, and biogeochemical states and processes of headwater stream ecosystems relevant to California and (ii) evaluate the effects of forest restoration techniques including prescribed fire and mechanical thinning. While the foci of the two efforts are cross-disciplinary, here we showcase the SSCZO–KREW

observatory via a hydrological perspective. Pertinent hydrological questions include the following:

1. How do regolith properties vary over 10-m to 100-km scales? This question of understanding regolith storage across climate (elevation) gradients is central to the regional understanding of climate–biota–regolith interactions.
2. How do physics, chemistry, and biology interact to influence critical-zone function over instantaneous to decadal timescales? Among others, this question focuses on how and where plant accessibility of stored water changes seasonally and during drought including associated feedbacks.
3. How do regolith development and properties control, limit, or modulate effects of climate change, forest management, or disturbance on hydrology, biogeochemistry, and ecology? As an example, this question addresses how surface and subsurface water budgets behave as a result of managed and natural disturbances such as fire, mechanical thinning, or forest die off and how this behavior influences water quality and supply, including to what extent have higher forest density conditions resulting from prolonged fire suppression affected ecosystem function and hydrology?
4. What measurements can best advance knowledge of the critical zone? The foundation for advances in the above questions rests on making appropriate, strategic measurements of the critical zone through long-term, intensive, and extensive baseline measurements as well as shorter-term project or campaign measurements.

◆ Site Characteristics

Sierra Nevada

The Sierra Nevada rises from near sea level, in California's Central Valley, to over 4400 m. The mountain range extends across 70,000 km² with an asymmetric shape consisting of a gradually sloping western face and a steep eastern escarpment. This asymmetry is thought to be a result of uplift and tilting by compressional and extensional geologic forces over the last several tens of million years (Harden, 2004). The crest is higher in the south because of greater uplift rates (Graham and O'Geen, 2016). As a result, altitudinal gradients are stronger in the southern Sierra Nevada where the SSCZO and KREW research sites are located.

Glaciers sculpted most of the high country (above ~1800 m) during the Pleistocene. The Sierra Nevada Batholith exposed during this process consists of granodiorite and other similar coarse-grained crystalline rocks. Meanwhile, rivers have carved V-shaped canyons into lower elevations of the western slope, creating a landscape of broad interfluves and adjacent deep valleys.

Mean annual precipitation ranges from <1 m in the south to >2 m in the north with a strong west–east gradient that increases with elevation to the crest and decreases again toward the eastern flank. Above an elevation of 1500 m, most precipitation falls as snow, while elevations below this zone receive precipitation as rain or snow that melts rapidly between storms. The soil moisture regime is mainly xeric at low–mid elevations, with a Mediterranean-type climate characterized by cool moist winters and warm dry summers, but udic at higher elevations where snowmelt and summer

thunderstorms keep the soil moist longer in summer. Air temperature also decreases as elevation increases, creating a thermic soil temperature regime in the foothills that transition to mesic and frigid at middle elevations and cryic at high elevation.

Vegetation on the west slope closely reflects variations in elevation and climate. Rising above agricultural lands of the Central Valley, naturalized annual grasslands merge into oak savannah and oak woodlands of the foothill region. Foothills extend to \sim 600 m elevation in the northern Sierra Nevada and 1500 m in the southern part of the range. As elevation increases, foothills transition to mixed-conifer forests. Subalpine forest is typically found at elevations above 2700 m.

Study Sites

The study area is located on the western slope of California's southern Sierra Nevada, \sim 35 miles northeast of Fresno, CA, between $37^{\circ}6.484'$ N, $119^{\circ}43.949'$ W and $37^{\circ}4.088'$ N, $119^{\circ}11.665'$ W. Five sites, spanning a 2300-m elevation range, exploit gradients in climate, regolith, soils, and vegetation (Fig. 1). The five combined SSCZO and KREW sites include the following: (i) rain dominated oak savannah (San Joaquin Experimental Range), (ii) rain dominated pine-oak forest (Soaproot catchment), (iii) rain-snow coniferous forest (Providence catchments), (iv) snow-dominated coniferous forest (Bull catchments), and (v) snow-dominated subalpine forest (Short Hair) (Fig. 1 and 2). Soil landscapes have similar age except for the highest elevation, which is younger where bedrock was scoured by glaciers during the last glacial maximum (Giger and Schmitt, 1993). Sites along the elevation transect capture the systematic variation in climate and vegetation that exist along the

west slope of Sierra Nevada. Thus, these five sites are representative of the hydrology, soils, and biophysical conditions throughout the southern Sierra and serve as a platform to extrapolate findings across the region (Dahlgren et al., 1997).

The oak savannah site is located at the San Joaquin Experimental Range and spans elevations of 210 to 520 m ($37^{\circ}6.484'$ N, $119^{\circ}43.949'$ W; https://www.fs.fed.us/psw/ef/san_joaquin/) (Fig. 1 and 2). It represents the driest and warmest site, with a mean annual temperature (MAT) of 16.6°C and mean annual precipitation (MAP) of 513 mm yr^{-1} . Vegetation consists of scattered blue oak (*Quercus douglasii* Hook. & Arn.) and interior live oak (*Quercus wislizeni* A. DC.) with naturalized annual grass understory. Soils are classified as Ahwahnee (coarse-loamy, mixed, active, thermic Mollic Haploxeralfs), Vista (coarse-loamy, mixed, superactive, thermic Typic Haploxerepts), or Auberry (fine-loamy, mixed, semiactive, thermic Ultic Haploxeralfs) series. The extent of weathering and pedogenesis is low. Soils are coarse textured (loamy sands and sandy loams), shallow to moderately deep (Beaudette and O'Geen, 2016). The site consists of rolling hills that serve as small, localized catchments (typically <1 ha) that feed ephemeral streams.

The pine-oak forest site is located at Soaproot Saddle with an elevation range between 1500 and 1000 m ($37^{\circ}2.4'$ N, $119^{\circ}15.42'$ W). This site is situated at the lower boundary of the rain-snow transition line (Fig. 1 and 2). It is representative of a midmontane, mixed-conifer ecosystem exhibiting high net primary productivity and strong seasonality with warm dry summers and cool wet winters. The MAT is 13.8°C and MAP is 805 mm yr^{-1} (Goulden et al., 2012). The site consists of a mix of ponderosa pine (*Pinus ponderosa* Lawson & C. Lawson), California black oak (*Quercus*

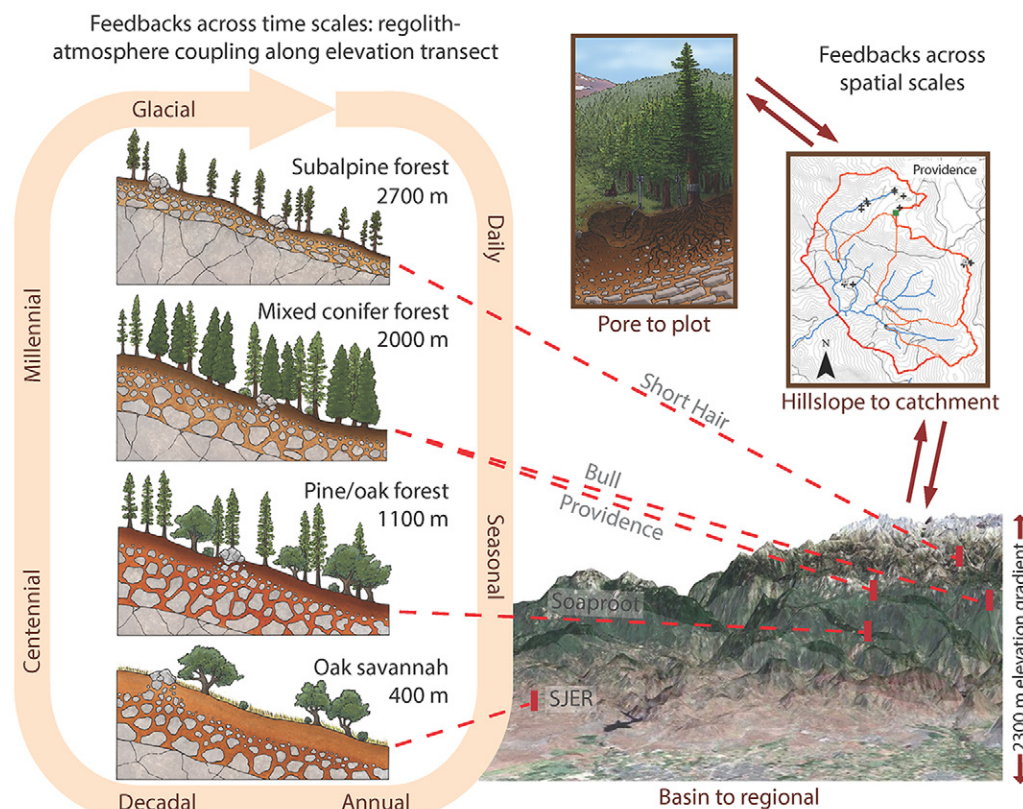


Fig. 1. The Southern Sierra Critical Zone Observatory and Kings River Experimental Watersheds have hydrologic observatories spanning a 2300-m elevation range. The mixed-conifer forest site at Providence (middle) is the most heavily instrumented site with three gaged headwater catchments nested within a fourth gaged catchment. Illustrations by Jenny Park.

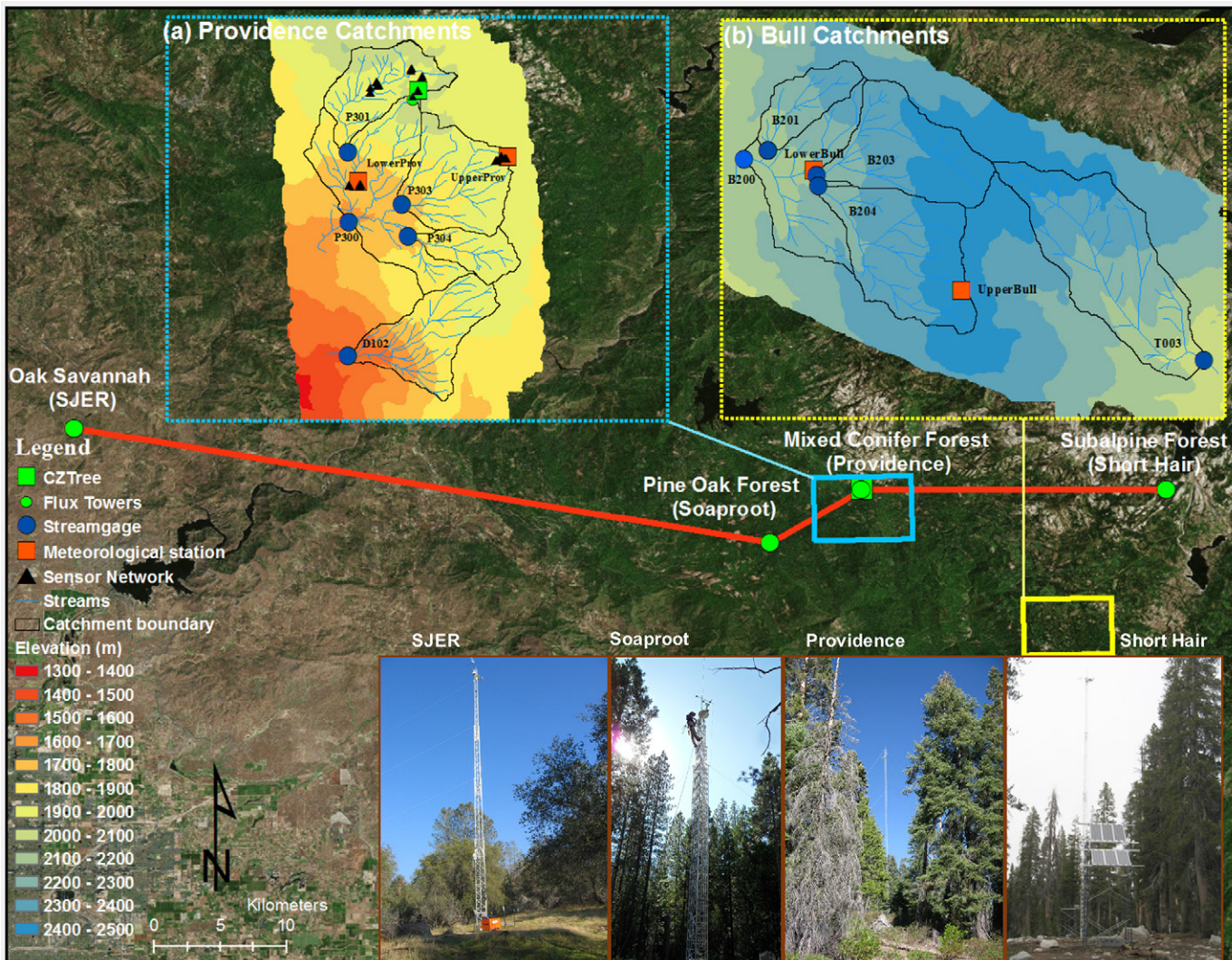


Fig. 2. Monitoring networks in and around Providence and Bull Creek catchments, and the Southern Sierra Nevada Critical Zone Observatory flux tower transect. Site names correspond to vegetation types: SJER, oak savannah; Soaproot, pine oak forest; Providence, mixed-coniferous forest; Short Hair, subalpine forest.

kelloggii Newberry), and incense cedar [*Calocedrus decurrens* (Torr.) Florin]. Soils are mapped at the family level, consisting mainly of Holland (fine-loamy, mixed, semiactive, mesic Ultic Haploxeralfs) and Chaix (coarse-loamy, mixed, superactive, mesic Typic Dystroxerepts) series, which are representative of soils across a similar elevational band of the western Sierra Nevada. Holland has sandy loam surface texture and underlying Bt horizons with sandy clay loam textures. It is a highly weathered Ultic Halploxeralf. Red hues indicate abundance of hematite, which is indicative of a relatively intense degree of weathering. The Chaix series has sandy loam textures throughout the profile. This soil is found on landscape positions that shed water and sediment, thus erosion outpaces soil development. The site is a 543-ha headwater catchment. Most of the hydrological monitoring infrastructure is located within the footprint of the eddy flux tower.

The rain–snow mixed-conifer forest site (Providence catchments) is the primary SSCZO–KREW research area located

mostly at Providence Creek, a tributary to the North Fork of the Kings River (Fig. 1 and 2). The 4.6 km² Providence Creek catchment (P300) ranges in elevation from 1660 to 2115 m (37°3.120' N, 119°12.196' W at P300 gauging station). Nested within the P300 catchment are three subcatchments designated as P301, P303, and P304. The Duff Creek (D102) catchment is adjacent to P300, has similar site conditions, an elevation of 1524 to 1988 m, and is included in the rain–snow mixed-conifer study site. The MAT is 8°C and MAP is 1015 mm yr⁻¹. The site is largely mixed-coniferous forest (76 to 99%) with some mixed chaparral and barren land cover. Sierran mixed-conifer vegetation in this location consists largely of white fir [*Abies concolor* (Gord. & Glend.) Lindl. ex Hildebr.], ponderosa pine, Jeffrey pine (*Pinus jeffreyi* Balf.), California black oak, sugar pine (*Pinus lambertiana* Douglas), and incense cedar.

There are three main soil series mapped in the Providence catchments: Gerle (coarse-loamy, mixed, superactive, frigid Humic

Dystroxerepts) and Cagwin (mixed, frigid Dystric Xeropsammets) are found at higher elevations (1800–2400 m), and Shaver (coarse-loamy, mixed, superactive, mesic Humic Dystroxerepts) occurs at 1750 to 1900 m (Bales et al., 2011). Gerle and Cagwin have a frigid soil-temperature regime. Cagwin and Gerle series are classified as Dystric Xeropsammets and Humic Dystroxerepts, respectively. Cagwin tends to occur on erosive landscapes such as convex ridge tops, steep mountain slopes, and sparsely vegetated areas intermixed with rock outcrops. As a result, Cagwin is sandy with shallow and moderately deep phases and minimal horizon differentiation. Gerle series displays some initial stages of pedogenesis. It is very deep, well drained and formed in glacial till, glacial outwash, and alluvium derived primarily from granitic rocks. Shaver has a warmer (mesic) soil temperature regime compared with higher elevation sites. The profile shows initial stages of pedogenesis with sandy loam textures throughout and slight rubification and transformation of primary minerals.

The snow-dominated mixed-conifer forest site consists mostly of Bull Creek (B200) (2130–2498 m elev.; $36^{\circ}58.631' N$, $119^{\circ}4.917' W$) and a second set of nested catchments (B201, B203, and B204) (Fig. 2). One stream located in the Teakettle Experimental Forest (T003; 2062–2498 m elev.; <https://www.fs.fed.us/psw/ef/teakettle/>) is outside the Bull catchment but has similar attributes and is included in the snow-dominated mixed-conifer forest site. The MAT is $7.4^{\circ}C$ and MAP is 1386 mm (Safeeq and Hunsaker, 2016). Vegetation at the Bull site is similar to that at Providence but has higher concentrations of California red fir (*Abies magnifica* A. Murray bis), less California black oak, and no chaparral. Soils in the Bull catchments are predominately classified as the Cagwin series (Johnson et al., 2011).

The subalpine forest site (Short Hair) occupies the highest elevation at Short Hair Creek (2670 m) near Courtright Reservoir in Fresno County ($37^{\circ}4.049' N$, $118^{\circ}59.204' W$) (Fig. 1 and 2). The MAT is $4.2^{\circ}C$ and MAP is 1078 mm yr^{-1} (Goulden et al., 2012). The vegetation community is largely lodgepole pine (*Pinus contorta* Douglas ex Loudon) and western white pine (*Pinus monticola* Douglas ex D. Don). This site has a cryic soil temperature regime and udic soil moisture regime. The site has thin patchy and rocky soils that limit moisture storage intermixed with areas of deep glacial till. Soils are mapped as the Stecum series (sandy-skeletal mixed Typic Cryorthents). This site was glaciated in the Pleistocene resulting in hard weathered bedrock (WB) underlying soil (Gillespie and Zehfuss, 2004). The site represents a headwater catchment, and the hydrological monitoring infrastructure is located within the footprint of the eddy flux tower.

Basic Long-Term Observations

Most of the long-term observations of this hydrological observatory are located at the two mixed-conifer sites—lower elevation Providence and higher elevation Bull—strategically placed to capture the rain–snow transition zone and seasonal snow zone (Fig. 2). Johnson et al. (2011) and Safeeq and Hunsaker (2016) provide detailed information on physical and chemical properties

of Providence and Bull catchments. Here we provide an overview of long-term observations at the two sites.

Meteorology and Precipitation Chemistry

Meteorological stations are located at upper and lower elevations in both Providence and Bull catchments. These meteorological stations were installed between 2002 and 2004 and consist of the following instruments: an alter-shielded weighing-bucket precipitation gauge (Belfort 5-780, Belfort Instruments, and 260-952 Alter-style wind screen, Novalynx Corporation), air temperature and relative humidity (HMP50, Vaisala), incoming solar radiation (CM3 Pyranometer, Kipp & Zonen), wind speed and direction (models 013 and 023, respectively, Met One Instruments), and an acoustic snow depth sensor (Judd Communications). Additionally, higher-elevation meteorological stations are each equipped with a 3.3-m snow pillow (Snowsaver) monitored with a Sensotec pressure transducer (Honeywell Inc.).

The KREW has been part of the National Atmospheric Deposition Program (NADP) National Trends Network since 2007, and site CA28 of the NADP network is colocated with the UpperProv meteorological station. A separate rain gauge measures precipitation and collects atmospheric deposition during periods of precipitation. Wet deposition samples are processed in the national laboratory for pH, electrical conductivity, calcium, magnesium, potassium, sodium, ammonium, nitrate, chloride, sulfate, and phosphate. Further details on chemical analysis available at National Trends Network (<http://nadp.slh.wisc.edu/data/sites/siteDetails.aspx?net=NTN&id=CA28>).

In terms of annual precipitation, there is small variation across the four meteorological stations, and the MAP ranges between 121 and 133 cm yr^{-1} despite a 670 m elevation difference between LowerProv and UpperBull (Fig. 2). However, the $2.5^{\circ}C$ difference in MAT between the UpperProv and UpperBull sites produces a strong difference in snow water equivalent. This mainly is due to the fact that 60 to 80% of annual precipitation in this region falls in winter at temperatures between -0.4 and $+2.4^{\circ}C$, and snow can occur across this range of temperatures (Jennings et al., 2018). Average temperature of wet days (precipitation >0 mm) varies from 2.0 to $2.4^{\circ}C$ in Providence to -0.68 to $0.39^{\circ}C$ in Bull. The higher peak in snow water equivalent at UpperBull extends the snow-covered period in late spring and early summer by ~ 40 d, providing meltwater for ET at higher elevation where soil storage capacity is LowerBull (Safeeq and Hunsaker, 2016).

Meteorological observations show evidence of the effects of microclimate on energy budget and snowmelt. Temperatures at lower elevation sites in both Providence and Bull were generally lower than high elevation sites in each catchment. The average difference in annual consecutive degree-days calculated using average daily air temperature (starting on 1 October) between the higher and lower elevation sites ranges from $2^{\circ}C$ at Bull to $3^{\circ}C$ at Providence (Fig. 3). This observed divergent response of air temperature with elevation is not uniform between minimum and maximum temperatures. Observed maximum temperature follows the expected elevational gradient with a lapse rate of

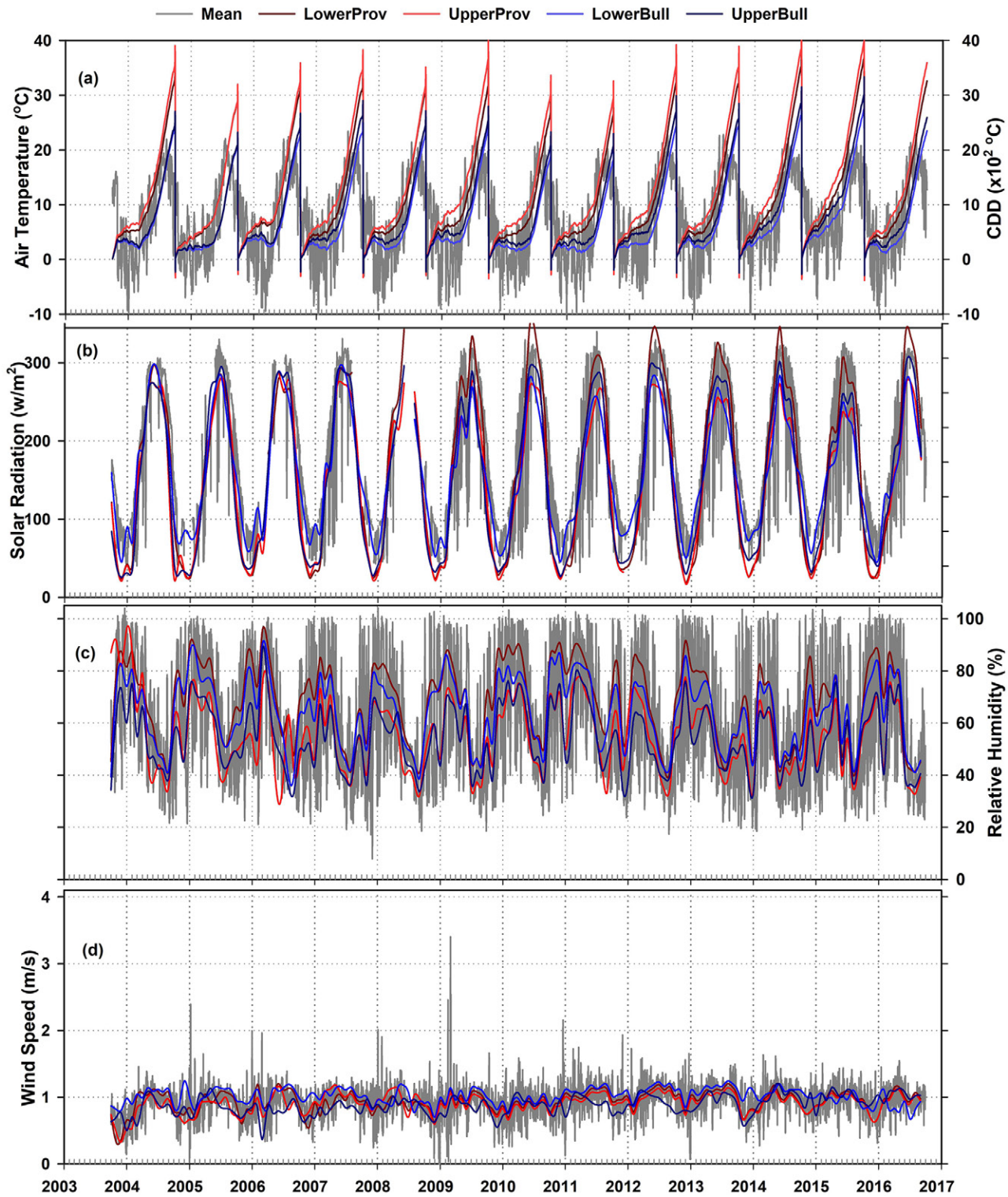


Fig. 3. Spatial pattern and long-term trends in (a) consecutive degree days (CDD) and monthly mean, (b) solar radiation (SR), (c) relative humidity (RH), and (d) wind speed across the four primary meteorological sites. Gray line shows mean, across the four sites.

$5.9^{\circ}\text{C km}^{-1}$, very similar to the standard wet adiabatic lapse rate of $5.0^{\circ}\text{C km}^{-1}$. However, minimum temperatures within each catchment are higher at high elevation stations, and increases are nearly $7.0^{\circ}\text{C km}^{-1}$. Some of this higher lapse rate for minimum temperatures is due to within-catchment trends in temperature.

The minimum average temperature across the two catchments declines with elevation from Providence to Bull at a rate of $5.9^{\circ}\text{C km}^{-1}$.

In terms of topographic differences, upper elevation sites are located on northwest aspects ($297\text{--}330^{\circ}$) with similar slopes

(17–22%). In contrast, LowerProv faces southwest (240°) on a slope of 7% and LowerBull is oriented toward the south (163°) with a slope of 19%. These differences in terrain parameters may be responsible for higher solar radiation at lower elevation than higher elevation sites. The lower minimum temperature and higher relative humidity at lower elevation sites are attributed to the sinking of cold air at night.

Discharge

Eight primary headwater catchments (P301, P303, P304, D102, B201, B203, B204, and T003) have been monitored by this hydrological observatory since October 2003, while two integrating catchments (P300 and B200) were gauged in October 2005 (Fig. 2). The T003 stream was first gauged in 1936 and monitored intermittently for periods of 3 to 12 yr since then until the KREW project took on monitoring in 2003. The range in catchment size is very similar between Providence (49–461 ha) and Bull sites (53–474 ha). The average slope of all gauged catchments ranges from 17 to 27%, with Providence catchments steeper than Bull catchments. All catchments have meadows, and the percentage of stream channel crossing a meadow varies between 0 (P303) to 16% (P301) in Providence and 23 (T003) and 92% (B201) in Bull.

Four Providence (P301, P303, P304, and D102) and three Bull catchments (B201, B203, and B204) are instrumented with large (30.5 or 61 cm) and small (8 cm) Montana flumes to capture the wide ranges in discharge. The T003 stream has a compound weir consisting of a 90° v-notch sharp-crested weir, a sharp-crested 0.61 by 1.83 m Cipolletti (trapezoidal) weir that activates at a stage of 91 cm in the v-notch, and a broad-crested rectangular weir that activates at the top stage (152 cm) in the sharp-crested weirs. Discharge has not exceeded the capacity of the sharp-crested weirs ($5.5 \text{ m}^3 \text{ s}^{-1}$) during the periods of measurement. The integrating sites are gauged with a 90° v-notch sharp-crested weir (P300) and a cross-section (B200) where a stage-discharge rating curve has been established using an acoustic Doppler velocimeter (SonTek, Inc.). At each flume or weir, stage is recorded using an ISCO 730 bubbler (Teledyne-ISCO) as a primary measure and either a capacitance probe (AquaRod, Geo Scientific) or a pressure transducer (Levellogger Edge M5, Solinst Canada Ltd, or Telog WLS-31, Trimble Water) as a secondary measure. The B200 stage is recorded with a pressure transducer.

Despite a similar precipitation amount, streamflow across the 10 gauging stations in our observatory is highly variable, driven by differences in the fraction of precipitation that falls as snow, regolith properties, and canopy cover (Fig. 4). The exception is P304, which has muted peak flow and sustained baseflow (Safeeq and Hunsaker 2016), possibly related to legacy gold mining operations. During the extended drought (2011–2016) P301 became an ephemeral stream because of a lack of subsurface storage that typically sustains baseflow. Comparing the two groups of catchments, minimum, mean, and maximum daily discharge was generally higher in Bull than Providence (Safeeq and Hunsaker, 2016). This difference was driven by both reduced ET and greater maximum snow pack and delayed snowmelt runoff at the higher elevation Bull sites.

Average annual ET declined by 45 mm km^{-1} increase in elevation, and this was consistent with the observed increase in discharge with elevation (49 mm km^{-1}) (Safeeq and Hunsaker, 2016). Reduced energy, lower vapor pressure deficits, and lower vegetation densities in Bull compared with Providence drive the reduction in ET. As noted by Safeeq and Hunsaker (2016), interannual variability in streamflow is smaller in Bull than in Providence, as the delayed snowmelt and lower ET rates in Bull allow greater carryover moisture storage for maintaining streamflow.

Water Quality

Just upstream of each of the 10 gauging stations is an optical turbidity sensor (DTS-12, Forest Technology Systems) and a flow triggered automatic pump sampler (Teledyne ISCO). Stream water samples collected from the automatic sampler during high flows, along with grab samples collected every 2 wk, are analyzed for suspended sediment concentration and water chemistry. While manual samples are collected year-round, automatic samplers are typically not operated during summer (July–September) because of very low flows (Hunsaker and Johnson, 2017).

The eight primary catchments are also equipped with sediment basins. Sediment accumulated in these basins is measured and removed each year. In most cases, sediment is weighed, but in large flow and sediment producing years, sediment is volumetrically surveyed and density samples are taken to determine the mass of sediment. Although some of this material is deposited, suspended sediment and organic matter, the majority is bedload sediment. Representative samples are analyzed for organic matter content and particle size distribution. Eagan et al. (2004), Hunsaker and Neary (2012), Stacy et al. (2015), and McCorkle et al. (2016) provide further details on sediment sampling and analysis.

Suspended sediment concentration in Providence catchments (85 mg L^{-1}) was, on average, higher than Bull catchments (44 mg L^{-1}) (Fig. 4C). At individual catchment level, suspended sediment concentration in P304 was highest (207 mg L^{-1}), followed by B201 (112 mg L^{-1}) and D102 (62 mg L^{-1}). The average (2003–2015) total annual mineral bedload sediment yield varied between $8.0 \pm 1.7 \text{ kg ha}^{-1}$ at Bull sites and $16.0 \pm 18.9 \text{ kg ha}^{-1}$ at Providence sites. Similar to suspended sediment, annual bedload yield in P304 (44 kg ha^{-1}) was four times higher than the next highest catchment (D102, 10.3 kg ha^{-1}). The bedload yields in P304 were also highly variable among years compared with other sites ($\text{SD } 56 \text{ kg ha}^{-1}$ in P304 vs. 16 kg ha^{-1} in D102). Despite a higher mean suspended sediment concentration in B201, annual bed load yield in that subcatchment was only 9 kg ha^{-1} and comparable with other Bull catchments.

Forest Fuel Reduction

Providence and Bull catchments are being used to evaluate forest management practices. Two of the eight primary catchments serve as controls (P304 and T003), while the rest were treated using mechanical thinning, prescribed burning, or a combination of thinning and burning (Fig. 2). Catchments P301, D102, B201, and B204 were mechanically thinned in the fall of 2012.

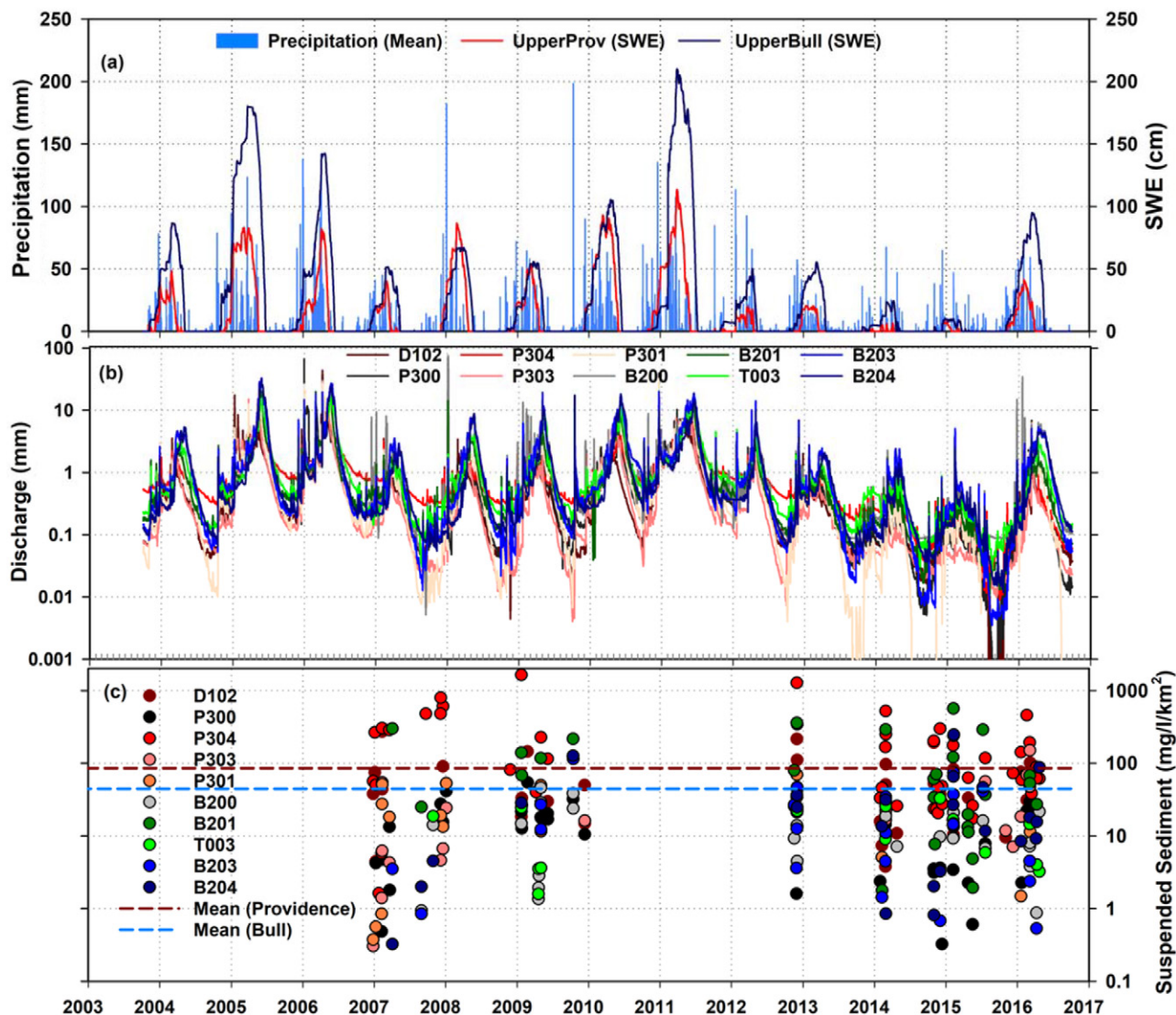


Fig. 4. Long term trends in (a) average daily precipitation (rain + snow) across sites and snow water equivalent (SWE) at UpperProv and UpperBull snow pillow sites, (b) daily streamflow (Q), and (c) event-based suspended sediment concentration (SSC). Mean SSC for five Providence (red) and five Bull (blue) catchments are shown as horizontal lines.

Two subcatchments from Bull (B203, B204) were burned in fall 2013 and two subcatchments from Providence (P301, P303) were burned in fall 2016. Vegetation plots (10 by 20 m) laid out on a grid ($n = 114$) were established in upland ($n = 114$) areas across the catchments and surveyed for understory and overstory structure and composition using a combination of line-intercept and belt-transect sampling. Surveys were conducted pre- (2004–2006) and post-treatment (2012–2014). Plots were resurveyed in summer of 2017 following the fire treatment in the Providence subcatchments and the expansive tree mortality during the recent California drought. Initial results indicate a 4 to 16% reduction in the basal area in thinned and thinned plus burned catchments relative to pretreatment condition, while in the control catchments, there were increases in basal area. Effects of forest fuel reduction from mechanical thinning and prescribed burning on water quantity and quality are currently being analyzed. However, considering

the extent of fuel reduction we hypothesize that the effects of the vegetation treatments on water quantity and quality will be very minimal. Historical data from paired-catchment studies suggest a minimum 20% reduction in forest cover for detecting a hydrologic change (Bosch and Hewlett, 1982).

Dedicated Long-Term Observations Evapotranspiration

Each of the four SSCZO sites along the elevation gradient has a set of shared measurements. Sites have an eddy-correlation flux tower to provide measurements of water, energy, and carbon exchange with the atmosphere (Fig. 5). Measurements on the towers include wind speed and direction, atmospheric water vapor flux, CO₂ flux, short- and long-wave radiation (incoming and outgoing), precipitation, relative humidity, and barometric pressure.

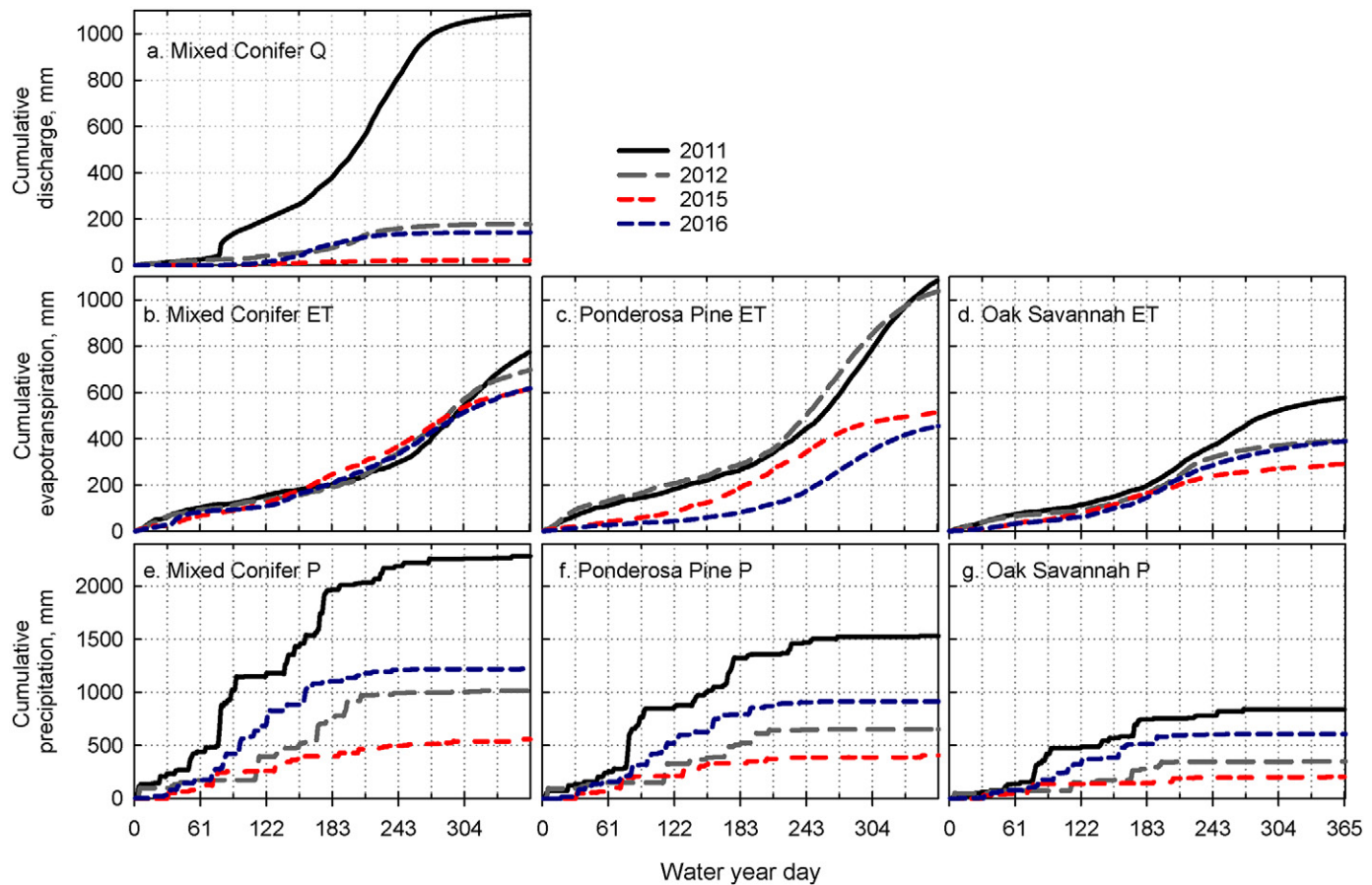


Fig. 5. Cumulative daily discharge from (a) P301, (b–d) evapotranspiration (ET), and (e–g) precipitation for 2011 through 2016 at mixed-coniferous forest (Providence), pine-oak forest (Soaproot), and oak savannah (San Joaquin). Time period represents 2 yr with high or average precipitation (2011 and 2016) and the multiyear drought 2012 through 2015. Subalpine forest was not included because the tower was damaged at this time by a fallen tree (adapted from Bales et al., 2018).

Altitudinal trends in ET are a result of precipitation, temperature, and vegetation. In 2011, a normal precipitation year, annual ET was highest at the pine-oak forest (Soaproot) site (1000 mm yr^{-1}) and decreased slightly at the mixed-conifer forest (Providence) ($\sim 750 \text{ mm yr}^{-1}$; Fig. 5). Evapotranspiration was much lower in oak savannah (San Joaquin site) ($\sim 525 \text{ mm yr}^{-1}$), which was the driest site (Fig. 5). Evapotranspiration was also low at the subalpine forest (Short Hair) because of low MAT at this high elevation ($\sim 520 \text{ mm yr}^{-1}$; data not shown, see Goulden et al., 2012).

Hydrologic and biophysical monitoring shows contrasting response to multiyear (2012–2015) drought conditions among sites (Fig. 5). Evapotranspiration remained high in the first year of drought at pine-oak forest then decreased. Evapotranspiration decreased all years in oak savannah. At the mixed-coniferous forest, however, the cumulative ET was more similar over the years because of more plant-available water as a result of relatively higher precipitation and large subsurface storage capacity. Storage may have remained high enough to meet forest demand because it experienced less drawdown because of lower ET relative to the pine-oak forest (Fig. 5b and 5c). Although the drought had no clear effect

on annual ET at the mixed conifer forest sites, stream discharge was exceptionally low, suggesting that the systems were experiencing severe drought stress (Fig. 5a). Moreover, precipitation in 2016 appears to have been primarily allocated to recharge of regolith storage capacity since stream flow remained low (Fig. 5a and 5e).

Evapotranspiration was initially highest in pine-oak forest site, but the high rate could not be maintained as drought progressed (Fig. 5). Despite low precipitation in 2012, annual ET remained high as a result of large plant-available water storage capacity of deep regolith. The pine-oak forest was unable to recover in 2016 in response to increased precipitation because of widespread tree death (Bales et al., 2018). During drought years, ET decreased earlier in the season at the oak savanna site. In 2016, a recovery in ET was observed at this site because annual grasses are less affected by antecedent moisture conditions.

Soil Water Dynamics

Each flux tower site has a minimum of three regolith profiles (soil + WB) instrumented with Decagon G3 sensors that measure soil moisture, temperature, and electrical conductivity (Meter Group). Regolith profiles also contain MPS-6 sensors (Meter

Group) to continuously measure water potential in soil and WB (Fig. 6). All sensors were placed at 50-cm depth intervals. The deepest sensor depth differed among sites because it reflected the depth at which hard bedrock was encountered, which varied among sites. At the oak savannah site, the deepest sensor depth was 200 cm. At the pine-oak forest site, the deepest sensor depth was 180 cm. At coniferous and subalpine forest sites, the deepest sensor depths were 235 and 110 cm, respectively. In areas that receive snow, sites have snowpack ultrasonic snow depth sensors (Judd Communications). The timeframe of this monitoring (water year [WY] 2016 and WY 2017) represents the recovery after the multiyear drought.

Despite large differences in precipitation, the general pattern of soil moisture dynamics was relatively similar across all sites as a result of the Mediterranean climate (Fig. 6). The period of water deficit in soil (summer months) was longest at lower elevations and shortest at subalpine forest. Water content was flashy in soil and more uniform in deep WB. Deep sensors in WB at oak savannah and pine-oak forest were near the groundwater table, which may have kept water content high and stable relative to that of soil (Fig. 6A and 6B). Water potential sensors in soil showed lower values during the growing season at upper elevations (mixed-conifer forest and subalpine forest; Fig. 6C and 6D). This response may have been muted at oak savannah because of coarser texture and because the sensor placement (50 cm) was below the annual grass root zone (max rooting depth typically 30 cm) (Fig. 6A). Widespread tree mortality throughout the pine-oak forest resulted in less utilization, and thus, less soil water depletion leading to higher water potential compared with higher elevations where forest mortality from drought was much less (Fig. 6B) (Bales et al., 2018). Large decreases in water potential during summer were observed at high elevation sites where forest vegetation survived (Fig. 6C and 6D).

Sensor Networks

Multiple instrument clusters quantify soil water storage in the Providence catchment (Fig. 2). Two sensor networks were installed near LowerProv and UpperProv meteorological stations in 2007 to 2008, clustered by aspect and with respect to distance from trees (open, drip-edge, and under-canopy). LowerProv has 10 instrument cluster nodes, with five each at north- and south-facing aspects. UpperProv has 17 nodes, with seven in north-facing clusters, five in south-facing clusters and five on flat ground. Another sensor network with 23 nodes was installed at P301 in 2011. Sensor nodes were placed in five distributed locations with respect to aspect in uplands, canopy coverage, and meadows. Upland sensors around trees were placed in open areas with no canopy coverage, under canopy, and at the drip edge of the canopy.

Each instrument cluster node measures snow depth, relative humidity, air temperature, soil moisture, and soil temperature. Snow depth was measured with ultrasonic depth sensors mounted 3 m aboveground (Judd Communications). Air temperature and relative humidity are measured with Sensiron SHT15 in a Davis 7714 radiation shield (EME Systems). Soil moisture sensors

(ECH_2O -TM, METER Group) were placed at depths of 10, 30, 60, and 90 cm below the soil surface.

At the nodes collocated with the UpperProv and LowerProv mixed-conifer forest sites, changes in the seasonal signature of water storage reflect drought and diminished snowpack (Fig. 7). Seasonal replenishment of soil moisture supply was largest in years where snowpack was greatest. While recharge of soil moisture storage capacity occurred each year, the magnitude of stored water decreased as drought progressed. The duration of water deficit during late spring, summer, and fall months became progressively larger with each drought year. While snowpack was lower and more ephemeral at the LowerProv site, soil storage was higher at both north and south aspects because of finer soil textures (higher silt + clay) relative to UpperProv sites (Bales et al., 2011).

◆ Dedicated Campaigns and Experiments

The Southern Sierra Critical Zone Observatory Tree

In 2008, near the mixed-conifer forest eddy-flux tower in P301, the area underneath a white fir was instrumented with a multitude of sensors as part of a subsurface monitoring network (Fig. 8). The network monitors soil moisture (ECH_2O 5-TE and EC-TM, Meter Group, Decagon), matric potential (MPS-1, Decagon, and tensiometers), in addition to aboveground measurements of sap flow (TranzFlo heat pulse probes), trunk water content by time domain reflectometry, lower canopy air temperature using thermistors, and snow depth using ultrasonic sensors. A total of six soil profiles (see soil profiles in Fig. 8) were instrumented with water potential and volumetric water content sensors at depths of 15, 30, 60, and 90 cm. At the 30-cm depth, a radial array of 72 locations measured water potential and volumetric water content (MPS-1 in Fig. 8; radius = 5 m; sensors spacing = 80 cm). Three deep regolith profiles were instrumented with water content and water potential sensors at depths of 150, 200, and 250 cm.

This setup was designed to monitor surface and subsurface water budgets, with specific attention to moisture and temperature variability in near-surface soils. The SSCZO tree research has provided a detailed view of water use by trees in these mid-elevation Sierra Nevada forests. Combined with intensive measurements from the flux tower and subsurface exploration, we found that trees at this elevation access water from much deeper sources than previously thought and transpire through much of the winter (Bales et al., 2011; Goulden et al., 2012).

A key finding from the SSCZO tree was evidence of an upward gradient of water from deep regolith when overlying soils became dry. Each water year, there was a point in time at which water potential values at soil depths at 150 cm became more negative than the underlying regolith at 200 and 250 cm, indicating a transition from dominantly downward flow to a subsequent period of upward water movement by capillary flow (Fig. 9). This point in time was defined as the crossover point. This phenomenon of changing soil water

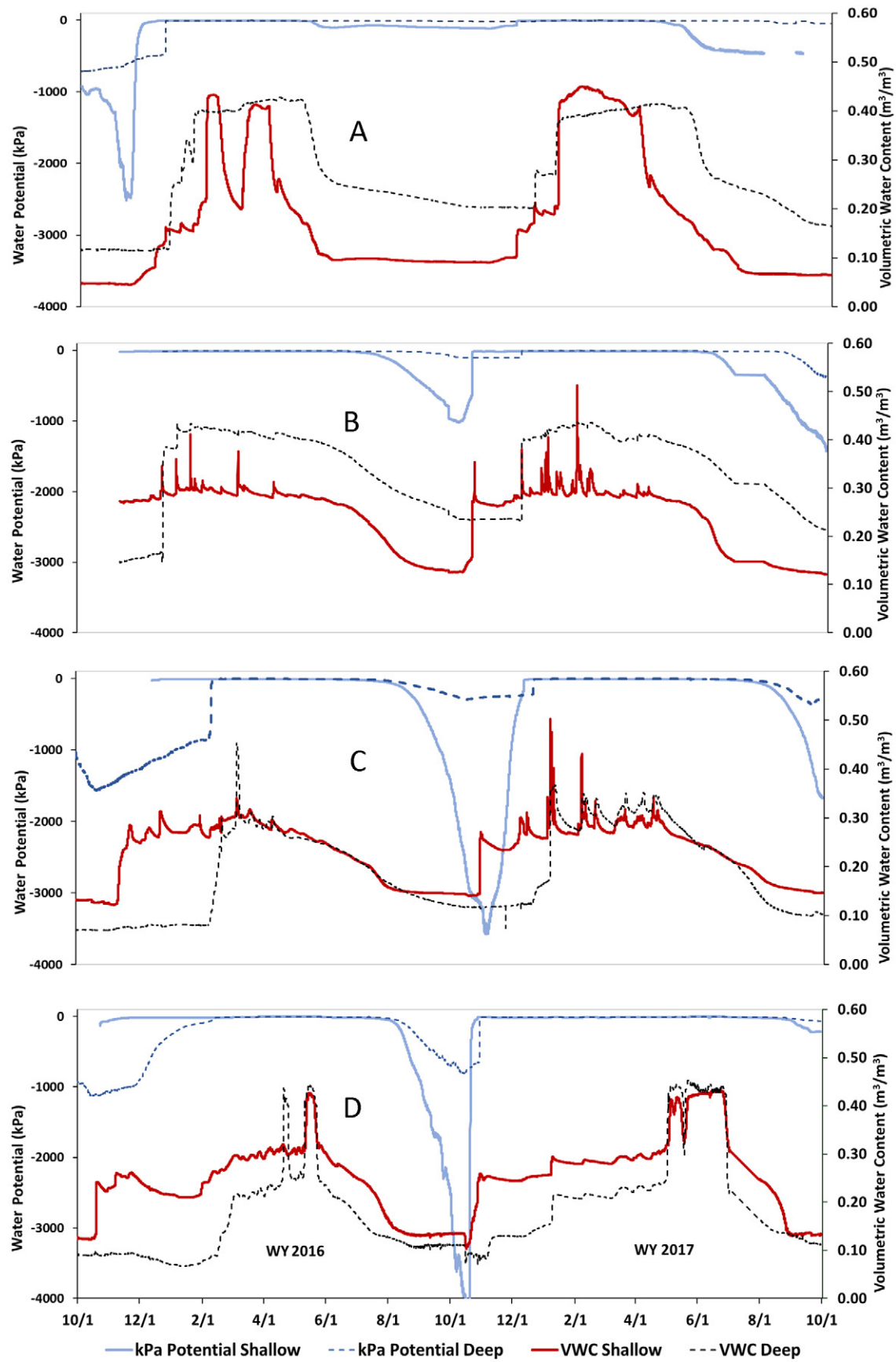


Fig. 6. Trends in water content and water potential located at shallow depths in soil (50 cm) vs. deep depths in weathered bedrock at the four SSCZO sites: (A) oak savannah, (B) pine-oak forest, (C) mixed-conifer forest, and (D) subalpine forest. Weathered bedrock sensor depths (Deep) differ among sites because of differences in soil thickness: A = 2.0 m, B = 1.8 m, C = 2.5 m, and D = 1.3 m.

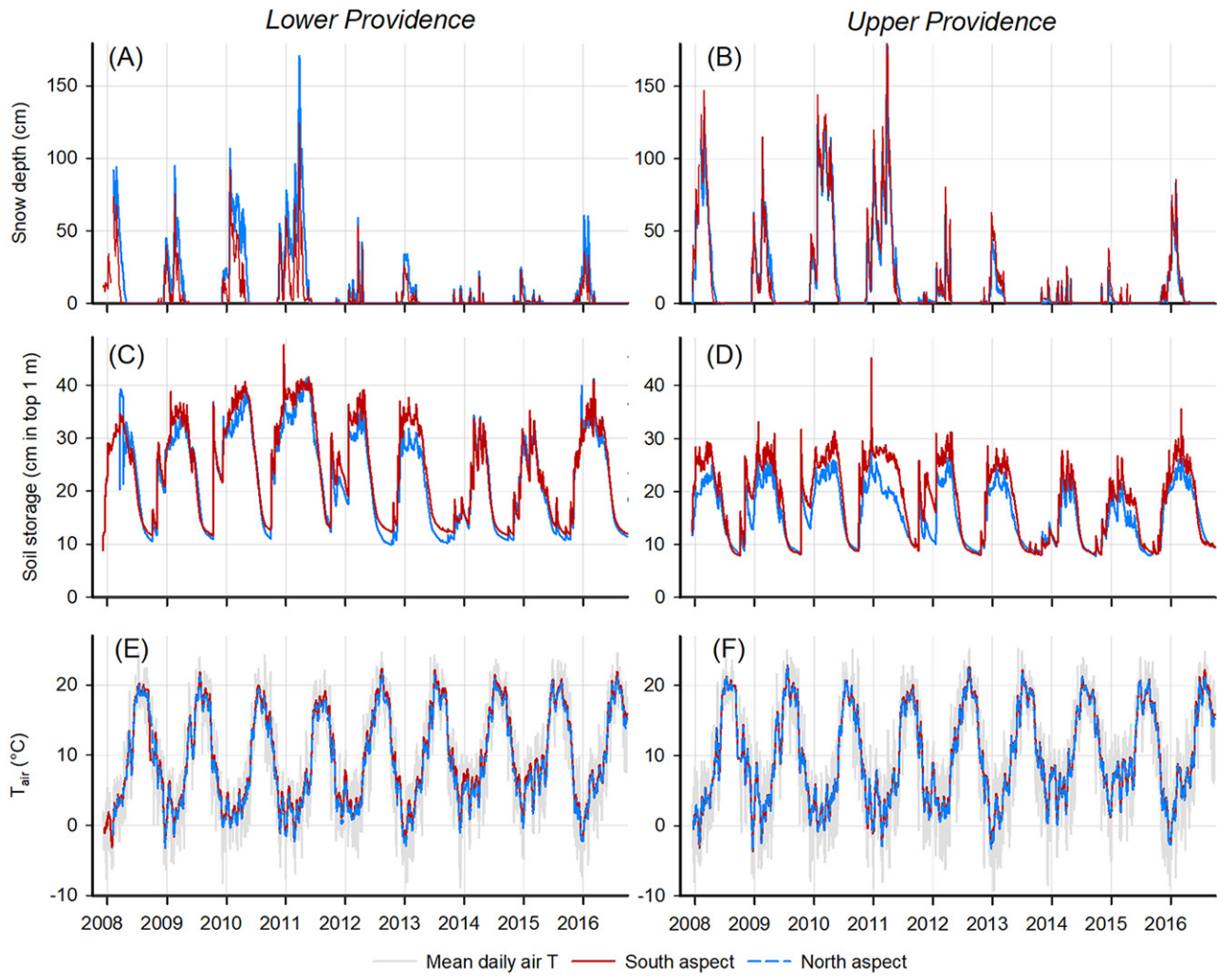


Fig. 7. Distributed sensor nodes track (A,B) snow depth, (C,D) soil moisture content, and (E,F) air temperature at meteorological stations at upper and lower elevations of mixed-coniferous forest (Providence). Comparison of upper and lower elevation sites include aspect Lower North ($n = 5$), Lower South ($n = 5$), Upper North ($n = 7$), and Upper South ($n = 5$). Air temperatures are smoothed with a 15 d running average with truncated ends and presented over daily mean values.

flow direction with crossover points occurred earlier each year as the drought progressed from 2011 to 2013 (Fig. 9). This crossover occurred in mid-August for WY 2011, whereas subsequent crossover points for WYs 2012 and 2013 were mid-July and mid-June, respectively. The earlier timing of crossover within the 3-yr observation period coincided with decreased precipitation for the respective WYs, thereby leading to decreased soil water storage. Consequently, trees depended on deeper subsurface water storage earlier in 2012 and 2013 than the 2011 WY, leading to upward capillary flow from deep regolith upward to the rooting zone.

Spatial Trends in Regolith Thickness and Storage

Deep-water storage is essential to the health and survival of Sierra Nevada forests (Hubbert et al., 2001). Regolith at some sites has been observed to extend several meters (Holbrook et al., 2014). There is limited knowledge of spatial patterns in regolith thickness because soil surveys do not normally document soil thickness beyond a depth of 2 m. A sampling campaign was organized to

document trends in regolith thickness (soil + WB) across the SSCZO gradient. We sampled regolith with a Geoprobe 7822DT rig (Geoprobe Systems) and hand augers in locations inaccessible by the Geoprobe. The Geoprobe is a tractor-mounted direct push drill capable of obtaining regolith depth measurements in excess of 10 m and was used at sites that were accessible with a tractor. Hand auger sampling was conducted from either the mineral soil surface, to consolidated hard bedrock, or at a maximum depth of 7.56 m, whichever was shallower. At lengths beyond 7.56 m, it became physically impractical to operate the hand auger.

Spatial trends in regolith thickness demonstrate a systematic change in water storage capacity, which is limited at high and low elevations. Observations demonstrate weathered-bedrock thickness is constrained by precipitation at low elevation oak savannah (San Joaquin Experimental Range) and low temperature and glaciation at high elevation subalpine forest (Short Hair) (Fig. 10). At oak savannah, regolith thickness was uniformly low, with a median thickness of 1.5 m. Median regolith thickness exceeded 5 m at most elevations at

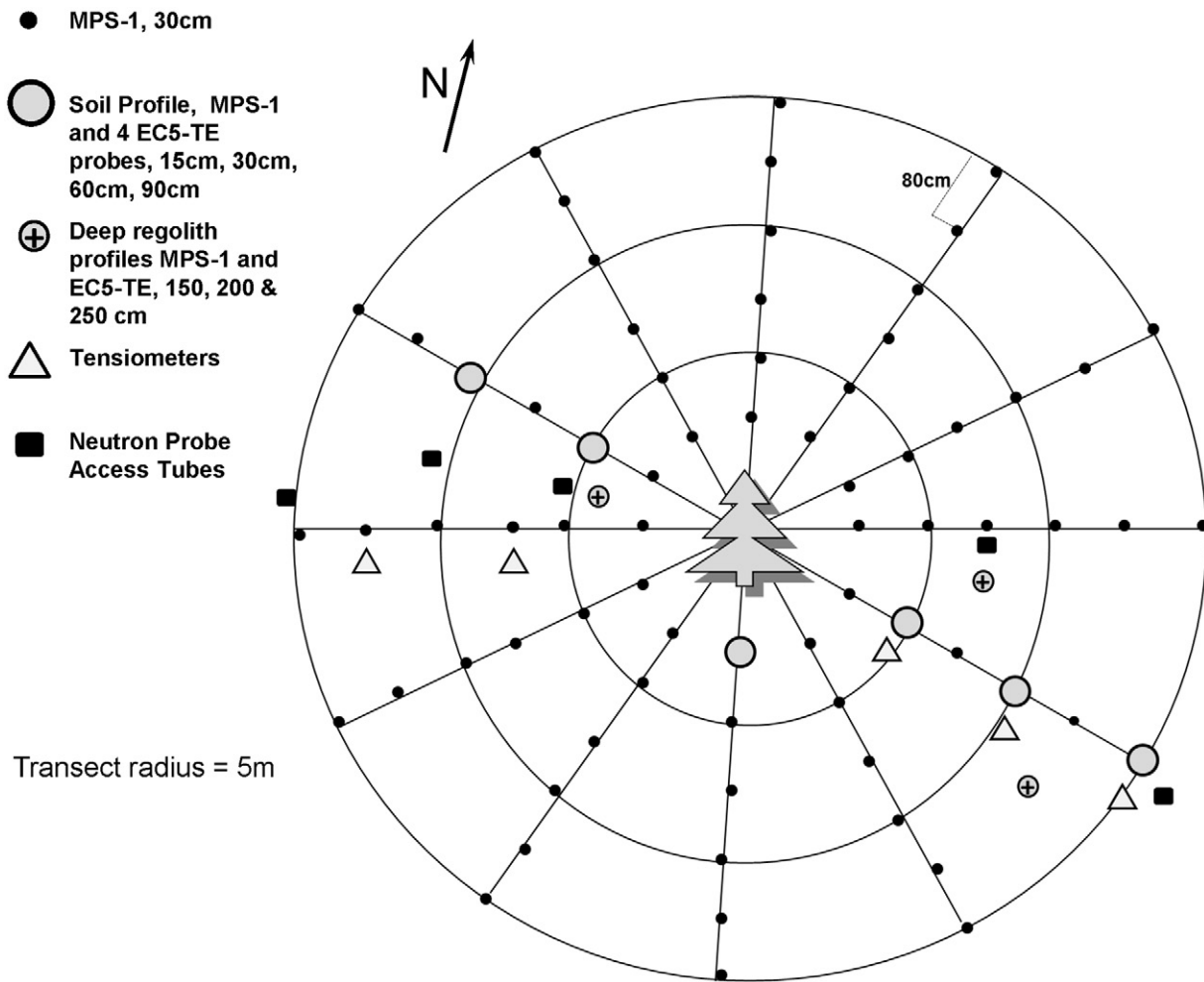


Fig. 8. Schematic of the sensor network established to monitor water dynamics in soil and deep regolith under the canopy of the Southern Sierra Critical Zone Observatory's experimental tree.

pine-oak forest (Soaproot). In the mixed-conifer forest (Providence), the median thickness decreased to 1.5 m, but was highly variable with the deepest observations exceeding 10 m. Subalpine forest had the most uniform regolith thickness with a median of 1.5 m, although sample size was much smaller ($n = 4$) (Fig. 10).

Table 1 highlights the relevance of documenting water storage capacity below soil. Plant available water holding capacity (PAW) was estimated in the Kings and San Joaquin River watersheds with two scenarios: (i) an estimate made directly from soil survey data, which does not account for storage below 2 m, and (ii) soil storage calculated from soil survey plus deep regolith storage derived from mean thickness across the area within three elevation bands (<600, 600–2000, and >2000) in the basins. Water retention curves generated from Tempe cells indicated that PAW of WB was $0.05 \text{ cm H}_2\text{O cm}^{-1}$ WB. The PAW of soil was calculated as a depth sum of soil horizons and an area weighted average of soil components within each map unit (including rock outcrop) using USDA-NRCS Soil Survey Geographic database (SSURGO) backfilled with USDA-State Soil Geographic database where SSURGO was missing. For Scenario 2, the PAW calculated from SSURGO

described above was added to the PAW (0.05 cm cm^{-1}) of deep regolith in instances where parathitic horizons (WB) extended to a 200-cm depth below 600 m elev., to 500-cm depth at elevations between 600 and 2000 m, and to 150-cm depth at elevations above 2000 m. If R horizons were mapped at any elevation, PAW was integrated to that corresponding depth.

Total storage nearly doubled in each river basin when considering the PAW of deep regolith (Scenario 2), from 0.25 to 0.45 km^3 at the Kings River Basin and 0.32 to 0.57 km^3 at the San Joaquin River Basin (Table 1). Both basins had a high percentage (>70% of elevation zone) of deep soils (Table 1) at 600 m and 600 to 2000 m elevation bands. These areas represent soil components that did not terminate with hard bedrock within the upper 1.5 m of soil, indicating storage capacity exists below this depth. Our deep coring observations suggest that deep regolith typically extends to <2 m at elevations below 600 m. This comparison of PAW shows major differences originating from the 600 to 2000 m elevation band where deep regolith is present (below a depth of 2 m), which occupies more of the land area in the San Joaquin River Basin (Table 1). These regional trends in

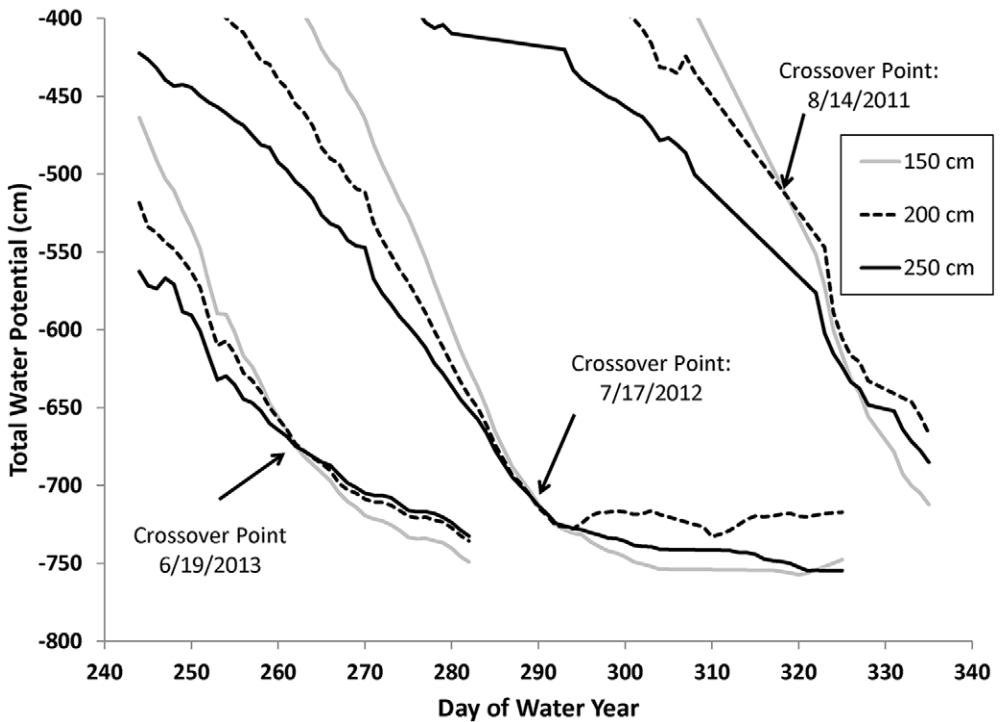


Fig. 9. Total soil water potential vs. day of the year in 2011, 2012, and 2013 at three depths in at the Southern Sierra Nevada Critical Zone Observatory Tree located in mixed-coniferous forest. Crossover points indicate when capillary rise from deep regolith could occur.

regolith storage may reveal important constraints on runoff generation and forest response to drought and climate change. For example, the extent of shallow soils at high elevations is linked to rapid response of stream flow to precipitation and snowmelt events because little storage exists to recharge (Fig. 6; Bales et al., 2011). Moreover, the extent of deep-water storage capacity may be linked to resilience to drought but also could cause forest overcrowding as a result of a water surplus. Overcrowding may lead to less resilience when storage is not replenished in multiyear drought as seen in 2015. Conversely, shallow regolith at high elevation may prevent upward migration of coniferous forest in response to global warming.

Monitoring Deep-Water Storage

Neutron probe access tubes were installed in triplicate for mixed-conifer forest, pine-oak forest, and oak savannah. Access tubes extend through soil to the contact between WB and hard bedrock. Monthly readings were recorded at 30-cm intervals in the upper 2.5 m and every 50 cm below 2.5 m to the depth of hard bedrock (between 9 and 10 m at the coniferous forest site). Monthly measurements were conducted during 2015, which was part of the multiyear drought. These measurements were compared with a one-time measurement in a wet year (May 2017), which was the earliest time mixed-conifer forest (Providence site) could be accessed after that winter because of prolonged snow pack (Fig. 11).

Volumetric water content during the year within the multi-year drought (2015) was exceptionally low and showed minimal differences between max, min, and mean values at all depths at all three sites (Fig. 11). Comparisons with soil moisture during a wet spring (2017) demonstrate that storage at depth at pine-oak forest (Soaproot Saddle) and mixed-conifer forest (Providence) had been

recharged. In the oak savannah (San Joaquin) site, similarities in water content at all depths in 2015 and 2017 show that this site has little water storage. At pine-oak forest and coniferous forest, volumetric water content remained at or below 10 cm in soil and WB throughout the 2015 water year. Recharge in 2017 increased water content to between 20 and 30 cm, and saturated conditions were present at the deepest depths. The difference between mean water content in 2015 and 2017 reflects a minimum estimate of plant-accessible water either via upward movement by capillary flow or direct uptake by deep roots.

Data Management and Policy

Data from the four SSCZO tower sites are publicly available through online data repository accessible at or through our digital data library (https://eng.ucmerced.edu/snsjho/files/MHWG/Field/Southern_Sierra_CZO_KREW). The SSCZO online data repository can also be browsed through the Southern Sierra Critical Zone Observatory (<http://criticalzone.org/sierra/data/datasets/>). Catchment streamflow and meteorological data from KREW are described by Hunsaker and Safeeq (2017, 2018). The KREW water quality data archives are being finalized and will be available on request from the US Forest Service Research and Development data archive (<https://doi.org/10.2737/RDS>). Data from the streamflow gauging stations, meteorological stations, instrument clusters, and flux towers are processed annually by water year for quality assurance, quality control, and gap filling. Data from campaigns and targeted studies are typically available after publication. Please inquire with the listed contacts for further information about potential access to data that are currently not publically posted.

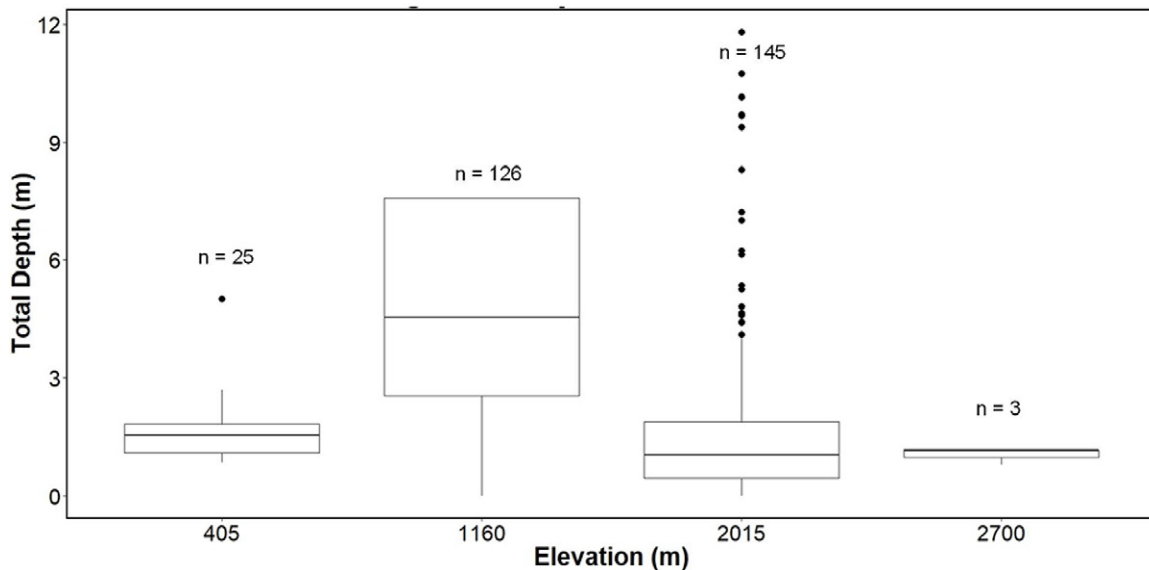


Fig. 10. Trends in regolith thickness across the elevation gradient of the Southern Sierra Critical Zone sites. Boxes show the first and third quartiles, lines inside the boxes indicate the median, whiskers give 95% confidence intervals, and points represent outliers. Maximum hand auger depths (7.5 m) were frequently encountered at 1000 to 2015 m elevations where terrain was inaccessible by Geoprobe.

New Insights and Novel Scientific Findings Plant-Accessible Water

In Mediterranean-type climates, precipitation typically falls when water demand by forests is low. High water demand occurs during the dry season, thus, forests rely on stored water

in soil and WB to survive (Arkley, 1981; Hubbert et al., 2001; Bales et al., 2011). The SSCZO discovered a large water storage capacity in deep regolith (soil + WB) (Holbrook et al., 2014; Klos et al., 2018), which has recently been identified at another critical zone observatory location (Rempe and Dietrich, 2018). There are also systematic trends in water storage capacity of regolith that extend across the Sierra Nevada

Table 1. Plant-available water storage scenarios calculated for Kings and San Joaquin river basins using (i) digital soil survey data and (ii) digital soil survey data plus estimates of regolith plant-available water holding capacity informed by regional trends in thickness across the Sierra Nevada.

Elevation zone	Area	Percentage of basin	Mean slope	Shallow soils†	Deep soils†	Unknown§	Non-soil¶	PAW soil survey#	PAW deep regolith††	MAP‡‡	April snowpack	PAW Scenario 1	PAW Scenario 2
m	ha	%			% elevation zone			cm				km ³	
Kings basin													
<600	21,552	5.4	17	8.9	72.1	8.2	10.8	11.9	16.4	60.6	0	0.03	0.04
600–2000	106,788	26.7	21	22.0	71.5	6.0	0.4	11.4	27.1	84.4	5.7	0.12	0.29
2000	271,675	67.9	20	62.4	20.1	17.3	0.3	3.9	4.4	102	65.4	0.11	0.12
Total	399,985	–	–	–	–	–	–	–	–	–	–	0.25	0.45
San Joaquin basin													
<600	41,748	9.6	10	9.7	82.9	2.0	5.3	10.8	14.9	51.9	0	0.05	0.06
600–2000	131,152	30.2	15	14.4	78.1	6.2	1.3	11.8	28.3	92.8	4.3	0.15	0.37
>2000	261,658	60.2	17	54.6	14.2	27.0	4.1	4.6	5.0	107	62.2	0.12	0.13
Total	434,558	–	–	–	–	–	–	–	–	–	–	0.32	0.57

† Proportion of soils with lithic contact (R within 50 cm) and rock outcrop.

‡ Proportion of soils that are clearly deeper than soil survey's maximum depth of investigation, that is, bottom horizons labeled Cr, C, BC, CB, or B.

§ Includes soils with unlabeled horizon names and map unit components classified at family level (i.e., not series). Also includes unsurveyed areas not backfilled with USDA State Soil Geographic database. The San Joaquin watershed includes 8766 ha of unsurveyed wilderness area.

¶ Non-soil includes lakes, urban land, and reservoirs.

Plant-available water holding capacity (PAW) calculated from USDA–NRCS Soil Survey Geographic database (SSURGO) for all available soil horizon data, including depths below 150 cm, where available, and is area weighted by major component percentage. All rock outcrop is assumed to have zero available water storage.

†† Plant-available water holding capacity (PAW) includes soil survey as described in previous footnote (#) plus an estimate of deep regolith where, where present, (i) paralithic horizons extend to 200-cm depth below 600-m elevation, 500-cm depth between 600 and 2000 m elevation, and to 150-cm depth above 2000 m elevation and where (ii) paralithic material is assumed to have 5% available water storage at depths where SSURGO data not available.

‡‡ MAP, mean annual precipitation and snowpack represent annual means from the California Basin Characterization model 1980–2010.

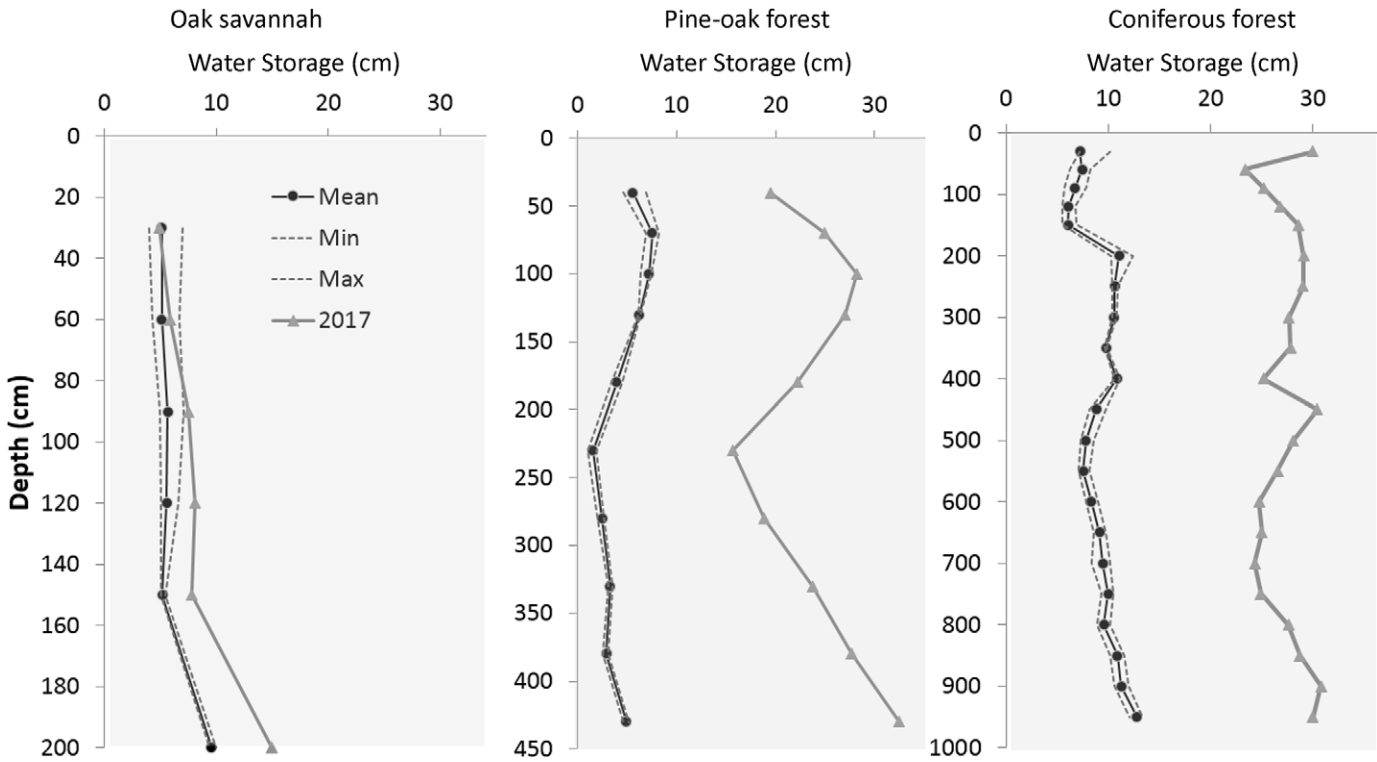


Fig. 11. Mean monthly neutron probe measurements of volumetric water content at oak savannah (SJER), pine oak forest (Soaproot Saddle), and mixed-coniferous forest (Providence [P301]) mixed-conifer forest during the last year of a multiyear drought (2015) relative to a one-time reading in spring 2017 after a wet winter. Note different scales on *y* axes.

(Fig. 9). The magnitude and spatial patterns of deep stored water is critical to understanding dynamics of the hydrologic cycle, ecological patterns within Sierra forests, and to predict effects of climate change.

Not all of the water stored in deep regolith can be reached by forest roots (Klos et al., 2018). Moreover, a significant fraction of stored water cannot be used by the forest because it percolates rapidly or is held too tightly in microscopic pore space (O'Geen, 2012). We are exploring techniques to document static and dynamic attributes of water and pore space in deep regolith presenting a framework to characterize stored water that integrates ecological and physical conditions of the critical zone. Five critical attributes of water (storage and utilization) in the critical zone were identified: dry-season water drawdown, dry-season available water, PAW, available water storage capacity, and total porosity (Klos et al., 2018). Consideration of these five attributes is necessary to fully comprehend hydrological and ecological processes in the Sierra Nevada.

Drought and Forest Health

Hydrologic monitoring during the 2011 to 2016 multiyear drought revealed feedback mechanisms that are important in predicting the influence of drought or warming on mountain runoff (Bales et al., 2018). Decreased precipitation and longer periods of sustained ET have reduced runoff by 30% relative to previous years. Warmer temperatures increased ET relative to previous years and reduced the amount of water in storage and streamflow by 5%. However, as

drought progressed, reductions in ET as a result of forest die off and fire increased the amount of water available for streamflow and soil storage (e.g., by 15% in 2016). Moreover, temperature limitations of ET at high elevation coupled with low water storage capacity in regolith at the subalpine forest maintained a continuous runoff supply (Bales et al., 2018). These offsetting feedbacks may not be as evident in basins that have more homogenous vegetative cover, smaller elevation ranges, or uniform regolith storage capacity.

Soil Moisture, Snowmelt, and Streamflow

The SSCZO monitoring network revealed patterns among aspects of the water balance. Streamflow becomes responsive to precipitation and snowmelt when soil water storage is high (>21 cm) (Bales et al., 2011). When soil water storage has been depleted, response of stream flow is muted, indicating that precipitation and snowmelt are being retained by capillary forces in soil. The replenishment of storage diminished by vegetation use during drought differs dramatically across the range of elevations of the SSCZO sites. Replenishment can take less than a year at high elevations where ET is low because of cool temperatures and where regolith is shallow. Replenishment may take several years at middle elevations (1100 m) where ET is highest, regolith is thick, and precipitation is moderate. However, recovery of regolith water storage at this elevation actually occurred sooner during the recent drought because of the diminished ET caused by extensive tree death (Bales et al., 2018).

Future Perspectives

Healthy Forests

Fire suppression has led to dense forests throughout much of the Sierra Nevada (Miller et al., 2009). High forest density increases competition for water among healthy trees and makes the forests highly susceptible to intense wildfire as well as diseases, pathogens, and insect outbreaks. Hydrologic feedbacks in the Sierra Nevada influence ecological patterns, biogeochemical cycles, and water availability for vegetation, wildlife, and critical downstream societal uses such as municipal water supply, power generation, and irrigation. Although we have made great progress in understanding some of the complex interactions among soils, vegetation, and climate, better information will be needed to make informed management decisions as the climate changes and the demand for water continues to increase (Bales et al., 2006).

Climate Change

Sierra Nevada snowpack is at risk as global temperatures rise (California Energy Commission, 2003). The southern Sierra Nevada is especially vulnerable because most large storms occur on days having temperatures between -3 and 0°C (Bales et al., 2006). Thus, a small increase in temperature will result in more rain and less snow. The full implications of this shift are not known because we do not yet completely understand the complex dynamics of water storage in the regolith. Is there enough regolith storage to store water that arrives as rain rather than snow? Would a switch from snowpack to regolith storage have similar feedbacks for stream flow? Where is regolith storage large enough to counteract flooding effects of episodic snowmelts? These types of questions, among many others, should be answered in order for Californians to better adapt to climate change.

References

- Arkley, R.J. 1981. Soil moisture use by mixed conifer forest in a summer-dry climate. *Soil Sci. Soc. Am. J.* 45:423–427. doi:10.2136/sssaj1981.03615995004500020037x
- Bales, R.C., M.L. Goulden, C.T. Hunsaker, M.H. Conklin, P.C. Hartsough, A.T. O'Geen, J.W. Hopmans, and M. Safeeq. 2018. Mechanisms controlling the impact of multi-year drought on mountain hydrology. *Sci. Rep.* 8:690. doi:10.1038/s41598-017-19007-0
- Bales, R.C., J.W. Hopmans, A.T. O'Geen, M. Meadows, P.C. Hartsough, P. Kirchner, C.T. Hunsaker, and D. Beaudette. 2011. Soil moisture response to snowmelt and rainfall in a Sierra Nevada mixed-conifer forest. *Vadose Zone J.* 10:786–799. doi:10.2136/vzj2011.0001
- Bales, R.C., N.P. Molotch, T.H. Painter, M.D. Dettinger, R. Rice, and J. Dozier. 2006. Mountain hydrology in the western United States. *Water Resour. Res.* 42:W08432. doi:10.1029/2005WR004387
- Beaudette, D.E., and A.T. O'Geen. 2016. Topographic and geologic controls on soil variability in California's Sierra Nevada Foothill Region. *Soil Sci. Soc. Am. J.* 80:341–354. doi:10.2136/sssaj2015.07.0251
- Bosch, J.M., and J.D. Hewlett. 1982. A review of catchment experiments to determine the effect of vegetation changes on water yield and evapotranspiration. *J. Hydrol.* 55:3–23. doi:10.1016/0022-1694(82)90117-2
- California Energy Commission. 2003. 2003 Integrated energy policy report: Climate change and California. Rep. 100-03-019. Calif. Energy Comm., Sacramento.
- Dahlgren, R.A., J.L. Boettinger, G.L. Huntington, and R.G. Amundson. 1997. Soil development along an elevational transect in the western Sierra Nevada, California. *Geoderma* 78:207–236. doi:10.1016/S0016-7061(97)00034-7
- Das, T., M.D. Dettinger, D.R. Cayan, and H.G. Hidalgo. 2011. Potential increase in floods in California's Sierra Nevada under future climate projections. *Clim. Change* 109:71–94. doi:10.1007/s10584-011-0298-z
- Das, T., E.P. Maurer, D.W. Pierce, M.D. Dettinger, and D.R. Cayan. 2013. Increases in flood magnitudes in California under warming climates. *J. Hydrol.* 501:101–110. doi:10.1016/j.jhydrol.2013.07.042
- Dettinger, M. 2011. Climate change, atmospheric rivers and floods in California: A multimodel analysis of storm frequency and magnitude changes. *J. Am. Water Resour. Assoc.* 47:514–523.
- Dolanc, C.R., H.D. Safford, J.H. Thorne, and S.Z. Dobrowski. 2014. Changing forest structure across the landscape of the Sierra Nevada, CA, USA, since the 1930's. *Ecosphere* 5:101. doi:10.1890/ES14-00103.1
- Eagan, S.M., C.T. Hunsaker, C.R. Dolanc, M.E. Lynch, and C.R. Johnson. 2004. Discharge and sediment loads at the Kings River Experimental Forest in the Southern Sierra Nevada of California. In: M. Furniss et al., editors, *Advancing the fundamental sciences: Proceedings of the Forest Service National Earth Sciences Conference*, San Diego, CA, 18–22 Oct. 2004. PNW-GTR-689. US For. Serv., Pac. Northwest Res. Stn., Portland, OR.
- Giger, D.R., and G.J. Schmitt. 1993. *Soil survey of Sierra National Forest*. US Govt. Print. Office, Washington, DC.
- Gillespie, A.R., and P.H. Zehfuss. 2004. Glaciations of the Sierra Nevada, California, USA. *Dev. Quaternary. Sci.* 2:51–62. doi:10.1016/S1571-0866(04)80185-4
- Goulden, M.L., R.G. Anderson, R.C. Bales, A.E. Kelly, M. Meadows, and G.C. Winston. 2012. Evapotranspiration along an elevation gradient in California's Sierra Nevada. *J. Geophys. Res.* 117:G03028. doi:10.1029/2012JG002027
- Goulden, M.L., and R.C. Bales. 2014. Vulnerability of montane runoff to increased evapotranspiration with upslope vegetation distribution. *Proc. Natl. Acad. Sci.* 111:14071–14075. doi:10.1073/pnas.1319316111
- Graham, R.C., and A.T. O'Geen. 2016. Geomorphology and soils. In: H. Mooney and E. Zalvadea, editors, *Ecosystems of California*. Univ. of California Press, Oakland.
- Griffin, D., and K.J. Anchukaitis. 2014. How unusual is the 2012–2014 California drought? *Geophys. Res. Lett.* 41:9017–9023. doi:10.1002/2014GL062433
- Harden, 2004. *California Geology*. 2nd ed. Pearson Education, Inc., Upper Saddle River, NJ.
- Holbrook, W.S., C.S. Riebe, M.L. Elwaseif, J. Hayes, K.L. Basler-Reeder, D. Harry, A. Malazian, A. Dosseto, P.C. Hartsough, and J.W. Hopmans. 2014. Geophysical constraints on deep weathering and water storage potential in the Southern Sierra Critical Zone Observatory. *Earth Surf. Processes Landforms* 39:366–380. doi:10.1002/esp.3502
- Howat, I.M., and S. Tulaczyk. 2005. Climate sensitivity of spring snowpack in the Sierra Nevada. *J. Geophys. Res.* 110:F04021. doi:10.1029/2005JF000356
- Hubbert, K.R., J.L. Beyers, and R.C. Graham. 2001. Roles of weathered bedrock and soil in seasonal water relations of *Pinus jeffreyi* and *Arctostaphylos patula*. *Can. J. For. Res.* 31:1947–1957. doi:10.1139/x01-136
- Hunsaker, C.T., and D. Johnson. 2017. Concentration–discharge relationships in headwater streams of the Sierra Nevada, California. *Water Resour. Res.* 53:7869–7884. doi:10.1002/2016WR019693
- Hunsaker, C.T., and D.G. Neary. 2012. Sediment loads and erosion in forest headwater streams of the Sierra Nevada, California. In: A.A. Webb, editor, *Revisiting Experimental Catchment Studies in Forest Hydrology*. Proceedings of a workshop held during the XXV IUGG General Assembly in Melbourne. June–July 2011. IAHS Publ., Wallingford, UK.
- Hunsaker, C.T., and M. Safeeq. 2017. Kings River Experimental Watersheds stream discharge. Forest Service Research Data Archive, Fort Collins, CO. doi:10.2737/RDS-2017-0037
- Hunsaker, C.T., and M. Safeeq. 2018. Kings River Experimental Watersheds meteorology data. Forest Service Research Data Archive, Fort Collins, CO. doi:10.2737/RDS-2018-0028
- Jennings, K.S., T.S. Winchell, B. Livneh, and N.P. Molotch. 2018. Spatial variation of the rain–snow temperature threshold across the Northern

- Hemisphere. *Nat. Commun.* 9:1148. doi:10.1038/s41467-018-03629-7
- Johnson, D.W., C.T. Hunsaker, D.W. Glass, B.M. Rau, and B.A. Roath. 2011. Carbon and nutrient contents in soils from the Kings River Experimental Watersheds, Sierra Nevada Mountains, California. *Geoderma* 160:490–502. doi:10.1016/j.geoderma.2010.10.019
- Klos, P.Z., M.L. Goulden, C.S. Riebe, C.L. Tague, A.T. O'Geen, B.A. Flinchum, M. Safeeq, M.H. Conklin, S.C. Hart, A.A. Berhe, P.C. Hartsough, W.S. Holbrook, and R.C. Bales. 2018. Subsurface plant-accessible water in mountain ecosystems with a Mediterranean climate. *Wiley Interdiscip. Rev.: Water* 5:e1277. doi:10.1002/wat2.1277
- McCorkle, E.P., A.A. Berhe, C.T. Hunsaker, D.W. Johnson, K.J. McFarlane, M.L. Fogel, and S.C. Hart. 2016. Tracing the source of soil organic matter eroded from temperate forest catchments using carbon and nitrogen isotopes. *Chem. Geol.* 445:172–184. doi:10.1016/j.chemgeo.2016.04.025
- Miller, J.D., H.D. Safford, M. Crimmins, and A.E. Thode. 2009. Quantitative evidence for increasing forest fire severity in the Sierra Nevada and southern Cascade mountains, California and Nevada, USA. *Ecosystems* 12:16–32.
- Miller, N.L., K.E. Bashford, and E. Strem. 2003. Potential impacts of climate change on California hydrology. *J. Am. Water Resour. Assoc.* 39:771–784. doi:10.1111/j.1752-1688.2003.tb04404.x
- Null, S.E., J.H. Viers, and J.F. Mount. 2010. Hydrologic response and watershed sensitivity to climate warming in California's Sierra Nevada. *PLoS One* 5:e9932. doi:10.1371/journal.pone.0009932
- O'Geen, A.T. 2012. Soil water dynamics. *Nat. Educ. Knowledge* 3:12.
- Rempe, D.M., and W.E. Dietrich. 2018. Direct observations of rock moisture, a hidden component of the hydrologic cycle. *Proc. Natl. Acad. Sci.* 115:2664–2669. doi:10.1073/pnas.1800141115
- Safeeq, M., G.E. Grant, S.L. Lewis, and C. Tague. 2013. Coupling snowpack and groundwater dynamics to interpret historical streamflow trends in the western United States. *Hydrol. Processes* 27:655–668. doi:10.1002/hyp.9628
- Safeeq, M., and C.T. Hunsaker. 2016. Characterizing runoff and water yield for headwater catchments in the southern Sierra Nevada. *J. Am. Water Resour. Assoc.* 52:1327–1346.
- Safeeq, M., S. Shukla, I. Arismendi, G.E. Grant, S.L. Lewis, and A. Nolin. 2016. Influence of winter season climate variability on snow–precipitation ratio in the western United States. *Int. J. Climatol.* 36:3175–3190. doi:10.1002/joc.4545
- Stacy, E.M., S.C. Hart, C.T. Hunsaker, D.W. Johnson, and A.A. Berhe. 2015. Soil carbon and nitrogen erosion in forested catchments: Implications for erosion-induced terrestrial carbon sequestration. *Biogeosciences* 12:4861. doi:10.5194/bg-12-4861-2015